Electrolyte Cation Dependence of the Electron Transfer Kinetics Associated with the $[SVW_{11}O_{40}]^{3-/4-}$ ($V^{V/IV}$) and $[SVW_{11}O_{40}]^{4-/5-}$ ($W^{VI/V}$) Processes in Propylene Carbonate

Jiezhen Li[a], Cameron L. Bentley[c], Tadaharu Ueda[d], Alan M. Bond[a,*] and Jie Zhang[a,b,*]

[a]School of Chemistry, Monash University, Clayton, Vic 3800, Australia

[b]ARC Centre of Excellence for Electromaterials Science, Monash University, Clayton, Vic 3800, Australia

[c]Department of Chemistry, University of Warwick, Coventry, CV4 7AL, U.K.

[d]Department of Applied Science, Kochi University, Japan

Corresponding authors: jie.zhang@monash.edu, alan.bond@monash.edu

Abstract

Changing the supporting electrolyte cation from tetrabutylammonium to 1-butyl-3-methylimidazolium is known to significantly increase the apparent heterogeneous electron transfer rate constants (k^0 value at the formal reversible potential (E_F^0)) associated with the $[SVW_{11}O_{40}]^{3-/4-}$ ($V^{V/IV}$) and $[SVW_{11}O_{40}]^{4-/5-}$ ($W^{VI/V}$) processes in aprotic organic media. In this study, supporting electrolytes containing 7 different cations, namely 1-ethyl-3-methylimidazolium ($[EMIM]^+$), 1-butyl-3-methylimidazolium ($[BMIM]^+$), 1-butyl-1-methylpyrrolidinium ($[Py_{14}]^+$), tetraethylammonium ($[TEA]^+$), tetrapropylammonium ($[TPA]^+$), tetrabutylammonium ($[TBA]^+$) and tetrahexylammonium ($[THA]^+$), have been investigated in order provide a systematic account of the influence of electrolyte cations on the rate of polyoxometalate (POM) electron transfer at a platinum disk electrode. Fourier transformed alternating current (FTAC) voltammetry has been used for the measurement of fast kinetics and DC cyclic voltammetry for slow processes. The new data reveal the formal reversible potentials and electron-transfer rate constants associated with the $V^{V/IV}$ (k_V^0) and $W^{VI/V}$ (k_W^0) processes correlate with the size of the supporting electrolyte cation. k_V^0 and k_W^0 values decrease in the order, $[EMIM]^+ > [BMIM]^+ > [Py_{14}]^+ \approx [TEA]^+ > [TPA]^+ > [TBA]^+ > [THA]^+$ for both processes. However, while k_V^0 decreases gently with increasing cation size (k^0 = 0.1 and 0.002 cm s^{-1} with $[EMIM]^+$ and $[THA]^+$ electrolyte cations, respectively), the decrease in k_W^0 is much more drastic (k^0 = 0.1 and 2×10^{-6} cm s^{-1} for $[EMIM]^+$ and $[THA]^+$, respectively). Possible explanations for the observed trends are discussed (*e.g.*, ion-pairing, viscosity, adsorption and the double-layer effect), with inhibition of electron-transfer by a blocking "film" of electrolyte cations considered likely to be the dominant factor, supported by a linear plot of $\ln(k^0)$ vs. $\ln(d)$ (where d is the estimated thickness of the adsorbed layer on the electrode surface) for both the $V^{V/IV}$ and $W^{VI/V}$ processes.

Graphical abstract

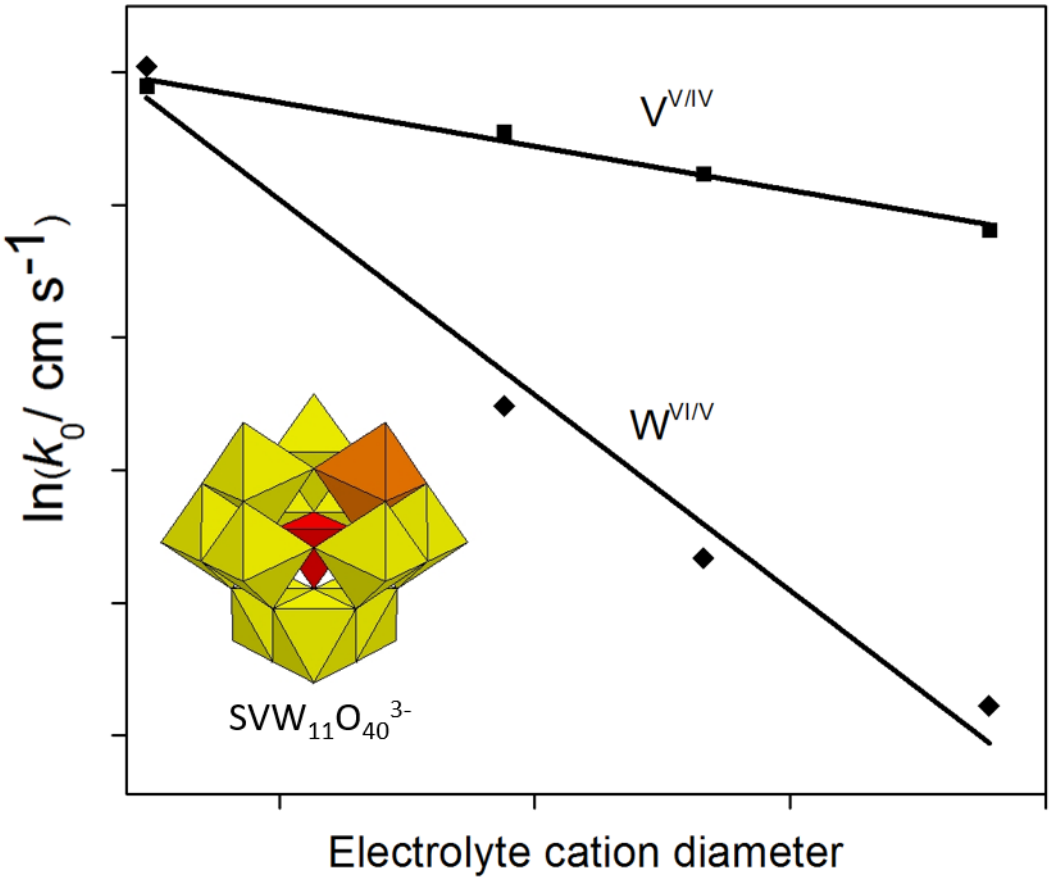

Keywords: electron transfer kinetics, polyoxometalates, propylene carbonate, cation dependence, Fourier transformed ac voltammetry

Introduction

It is of fundamental importance in electrochemistry to understand the factors that govern the rate of heterogeneous electron transfer. For an electrode reaction, this typically involves the transfer of charge (electrons) across an interface between a solid electrode and liquid electrolyte. It follows that the rate of electron transfer is governed by both the physicochemical properties of the electrode/electrolyte interface and the nature of the redox-active species. For an outer-sphere one electron transfer processes such as the reduction of $[Ru(NH_3)_6]^{3+}$ to $[Ru(NH_3)_6]^{2+}$ or the oxidation of ferrocene (Fc) to ferrenium cation (Fc^+), very similar electrochemical behavior is observed at Pt, Au, and carbon electrodes.[1, 2] However, the kinetics of the $Fe^{2+/3+}$ process, also considered to be an outer-sphere reaction in some studies, is much slower and differs markedly at these electrode materials.[3, 4]

The effects of the nature of the solvent (donor/acceptor or acid/base properties), supporting electrolyte and electrode material on electrode kinetics have been studied extensively.[5-12] For example, if the outer-shell contribution to the activation energy is the major factor governing the rate of electron transfer, the heterogeneous electron-transfer rate constant (k^0) exhibits a strong dependence on the properties of the solvent (dielectric constant).[13, 14] In addition, the rates of electrode reactions can be profoundly affected by the identity of the ions present in the supporting electrolyte[15-19]. For example, Peover and Davies[20] reported that the highly irreversible (kinetically sluggish) second step for reduction of 9,10-anthraquinone in dimethylformamide (DMF) can be made reversible (kinetically facile) through the addition of alkali metal ions. This effect was attributed to interactions (ion-pairing) between the semiquinone anion and the alkali metal cations.

Polyoxometalates (POMs) are anionic oxoclusters containing early transition metals in high oxidation states. They are nano-sized and display a wide variety of compositions and structures. They exhibit a wide range of properties, which have led to proposed applications in

diverse fields such as medicine, photochromic materials, solar energy, and so forth.[21-23] In particular, POMs can undergo fast, reversible and stepwise multielectron-transfer reactions without significant structural change, meaning they can be employed as catalysts for many redox reactions.[24-27] Furthermore, the properties of a POM, such as solubility, redox potential, and acidity can be finely-tuned by varying the constituent elements.[28]

The thermodynamic properties (formal reversible potentials, E_F^0) of POMs have been studied extensively.[28-30] For example, the electrochemical behaviour of $[Co_2W_{12}O_{42}]^{8-}$ was found to be highly solvent dependent.[31] The reversible potentials associated with these W-based redox centres shift negatively in a 50% mixed solvent aqueous electrolyte of dimethylformamide/water, acetonitrile/water or acetone/water compared to a pure aqueous electrolyte solution, while in dioxane/water mixtures, the processes shifted positively. The acidity of the media (proton availability) also influences the thermodynamic properties of POMs. Thus, while $[PMo_{12}O_{40}]^{3-}$ undergoes successive one-electron transfer processes in acetonitrile, the addition of acid causes a substantial change in reversible potential, so that when a high concentration is present, overall two-electron processes are detected.[32]

The kinetic properties (standard electron transfer rate constant, k^0 at E_F^0, and electron transfer coefficient, α) of POMs remain much less explored than the thermodynamic ones. Recently, we have reported a series of studies on the electrode kinetics of POMs.[33-36] In aqueous media, the k^0 values of the Keggin-type silicon tungstate POMs, $[SiW_{12}O_{40}]^{4-}$ and $[SiW_{12}O_{40}]^{5-}$, were found to be electrode material dependent.[33, 34] Much slower rate constants were found with boron-doped diamond (BDD) electrode compared to use of glassy carbon (GC) as the electrode material.[33] The effect of the electrolyte cation (Li^+, Na^+, K^+ and NH_4^+) on the electrode kinetics of these processes has also been studied[34]. In organic media (dimethylformamide) containing supporting electrolyte, the electrode kinetics associated with the $[SVW_{11}O_{40}]^{3-/4-/5-}$ processes are strongly dependent on the electrode

material as well as the ionic strength.[35] In our most recent study, we showed that changing the electrolyte cation from tetrabutylammonium to 1-butyl-3-methylimidazolium can significantly increase the electron-transfer kinetics of the $[SVW_{11}O_{40}]^{3-/4-/5-}$ processes at Pt, Au and BDD electrodes. We attributed this and other trends obvious to double layer effects and the nature of the electron-transfer processes (outer-sphere for the $V^{V/IV}$ reaction vs. inner-sphere for the $W^{VI/V}$ one).[36]

In the present study, our previous work is expanded systematically to provide a general account of the influence of electrolyte cations on the rate of POM electron transfer, using the $[SVW_{11}O_{40}]^{3-/4-/5-}$ reductive reactions as exemplar processes. The structure of $[SVW_{11}O_{40}]^{3-}$ [37] shown in Figure 1 shows the location of the V and W metal constituents. $[SVW_{11}O_{40}]^{3-}$ exhibits three well-defined one-electron reduction processes in molecular solvent (electrolyte) media.[37] The two initial processes, which are the focus for the current study, correspond to the reduction of V^{V} to V^{IV} (eq. 1) and W^{VI} to W^{V} (eq. 2).

$$[SV^{V}W_{11}^{VI}O_{40}]^{3-} + e^{-} \rightleftharpoons [SV^{IV}W_{11}^{VI}O_{40}]^{4-} \qquad (1)$$

$$[SV^{IV}W_{11}^{VI}O_{40}]^{4-} + e^{-} \rightleftharpoons [SV^{IV}W^{V}W_{10}^{VI}O_{40}]^{5-} \qquad (2)$$

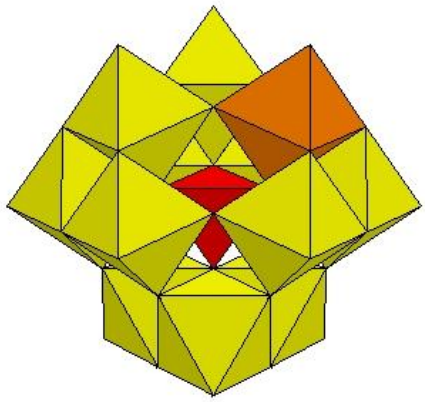

Figure 1. The structure of $[SVW_{11}O_{40}]^{3-}$. Color code: S (red), V (orange), W (yellow).[37]

Seven different electrolyte cations were used in this study, including imidazolium and tetraalkylammonium based cations (structures shown in Scheme 1). Salts containing large singly-charged cations such as tetraalkylammonium ions are commonly used for investigations

in dipolar aprotic solvents due to their relatively high solubility and weak tendency to form ion associates with anions in these systems. However, a number of studies has been reported which demonstrate that the electrode kinetics of can depend on the nature (size or structural symmetry) of the tetraalkylammonium cations.[38-41] For example, the rate constants (k^0 values) of a series of organic molecules have been shown to decrease with increase in the size of the alkyl group.[38] The solvent chosen in this study is propylene carbonate (PC), which has a high dielectric constant (64.9 at 25°C[42]), reducing the influence of ion pairing effects. Supporting electrolytes were added at a concentration of 0.5 M to provide a well-defined double layer. As is the case in our previous study, fast electrode kinetics were measured using large-amplitude Fourier-transformed alternating current (FTAC) voltammetry, which exhibits superior kinetic sensitivity in comparison with the conventional dc voltammetry[43] and slow processes were quantified by DC cyclic voltammetry using DigiElch digital simulation software package.

Scheme 1. Names, abbreviations and structures of the electrolyte cations used in this study.

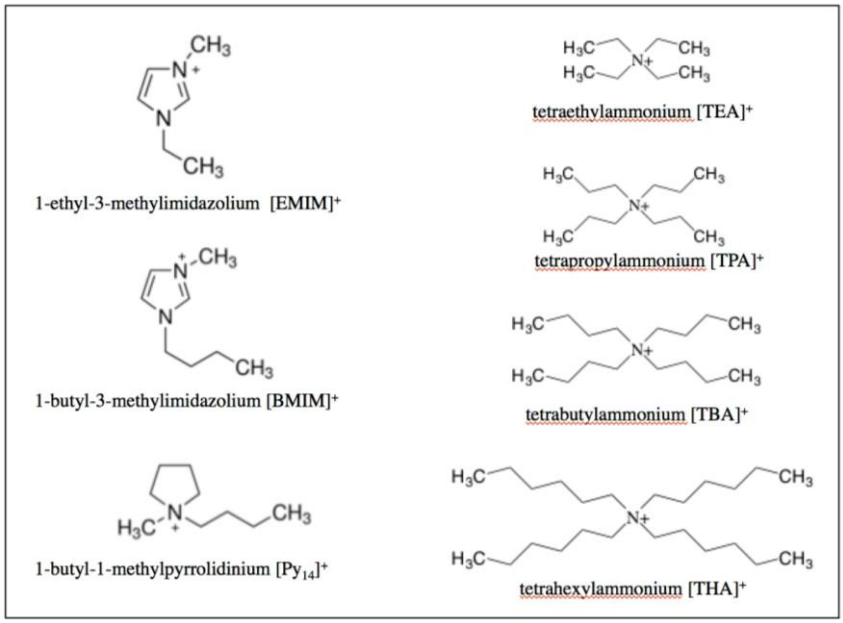

EXPERIMENTAL SECTION

Chemicals. Propylene carbonate (PC, 99.7%, Sigma-Aldrich), acetonitrile (CH_3CN, 97%, Sigma-Aldrich), ethanol (96%, Merck), 1-ethyl-3-methylimidazolium tetrafluoroborate ([EMIM][BF_4], 98%, Sigma-Aldrich), 1-butyl-3-methylimidazolium tetrafluoroborate ([BMIM][BF_4], 99%, IoLiTec), 1-butyl-3-methylimidazolium hexafluorophosphate ([BMIM][PF_6], 99%, IoLiTec), 1-butyl-1-methylpyrrolidinium tetrafluoroborate ([Py_{14}][BF_4], 99%, IoLiTec), tetraethylammonium tetrafluoroborate ([TEA][BF_4], 99%, Sigma-Aldrich), tetrabutylammonium hexafluorophosphate ([TBA][PF_6], 99%, Sigma-Aldrich) and tetrahexylammonium perchlorate ([THA][ClO_4]], 99%, Sigma-Aldrich) were used as received from the manufacturer. Ferrocene (Fc, Sigma-Aldrich, ≥ 98 %) was recrystallized from *n*-pentane (Merck) prior to use. Tetrapropylammonium tetrafluoroborate ([TPA][BF_4]) was prepared by a metathesis reaction between sodium tetrafluoroborate (Na[BF_4], Sigma-Aldrich) and tetrapropylammonium bromide ([TPA]Br, Sigma-Aldrich) in CH_3CN.

All electrochemical studies were carried out at 22 ± 2 °C using a standard three electrode electrochemical cell. Viscosity was measured using the falling ball method with an

Anton Paar automated microviscometer (AMVn). The working electrode was platinum (Pt, nominal diameter = 1.0 mm) or glassy carbon (GC, nominal diameter = 1.0 mm). Platinum wire was used for the auxiliary and reference electrodes. The quasi-reference electrode potential was calibrated against the recommended $Fc^{0/+}$ process." in the experimental section. Other experimental details are as reported elsewhere[36] and are summarized in the Supporting Information.

RESULTS AND DISCUSSION

DC Cyclic Voltammetric Characterization of the $V^{V/IV}$ and $W^{VI/V}$ Processes. The $[SVW_{11}O_{40}]^{3-/4-}$ ($V^{V/IV}$) and $[SVW_{11}O_{40}]^{4-/5-}$ ($W^{VI/V}$) processes were initially characterized by DC cyclic voltammetry at a Pt electrode. Verification of the first process as reduction of V^{V} to V^{IV} and the second more negative one to reduction of W^{VI} to W^{V} is given in reference.[37] Figure 2 shows a comparison of the DC cyclic voltammograms obtained from 1.0 mM $[SVW_{11}O_{40}]^{3-}$ in PC containing 0.5 M electrolytes outlined in Scheme 1, at a scan rate (v) of 0.1 V s^{-1}. Clearly, the formal reversible potentials (E_F^0) of the $V^{V/IV}$ and $W^{VI/V}$ processes, E_V^0 and E_W^0, are dependent upon the nature of the electrolyte. Slightly more positive E_V^0 and E_W^0 values are observed from [EMIM][BF_4] (0.316 V and -1.085 V, respectively) compared to [BMIM][BF_4] (0.306 V and -1.093 V, respectively). A larger variation is observed when using tetraalkylammonium cation as the cation constituent of the supporting electrolyte, with E_V^0 and E_W^0 shifting towards more negative potentials in the order of $[Py_{14}]^+ \approx [TEA]^+ > [TPA]^+ > [TBA]^+ > [THA]^+$. The negative shift in the E_F^0 values, as well as the increased potential gap separating the $V^{V/IV}$ and $W^{VI/V}$ processes (ΔE_F^0) is attributed to increasingly strong interactions between the electrolyte cation and the reduced form of the POM (*e.g.*, $[SVW_{11}O_{40}]^{4-}$) compared to the oxidized form of the POM (*e.g.*, $[SVW_{11}O_{40}]^{3-}$). It should be noted that because $[SVW_{11}O_{40}]^{3-/4-/5-}$ are all highly negatively charged species, the identity of the anion (*e.g.*, $[BF_4]^-$ vs. $[PF_6]^-$ vs. $[ClO_4]^-$) is not expected to influence electrochemical behavior as

confirmed by the fact that negligible differences in both reversible potentials and peak-to-peak separations was detected when using either [BMIM][BF_4] or [BMIM][PF_6] as the supporting electrolyte.

Table 1. DC cyclic voltammetric data derived at 22 ± 2 °C from the reduction of 1.0 mM $[SVW_{11}O_{40}]^{3-}$ in PC (0.5 M electrolyte) at a Pt macrodisk (diameter = 1.0 mm) electrode with a scan rate of 0.1 V s^{-1}.

Electrolyte	E^0_V(V)	$(\Delta E_p)_V$(V)	E^0_W(V)	$(\Delta E_p)_W$(V)	ΔE^0_F(V)
[EMIM][BF_4]	0.316	63	-1.085	65	1.400
[BMIM][BF_4]	0.306	67	-1.093	66	1.399
[BMIM][PF_6]	0.303	66	-1.090	68	1.393
[Py_{14}][BF_4]	0.333	76	-1.079	75	1.412
[TEA][BF_4]	0.342	79	-1.079	67	1.421
[TPA][BF_4]	0.309	82	-1.182	303	1.491
[TBA][PF_6]	0.254	88	-1.260	520	1.514
[THA][ClO_4]	0.214	110	-1.355	745	1.569

Another clearly evident feature is the electrolyte dependence of the DC voltammetric peak-to-peak separations, ΔE_p (= E_p^{Ox} - E_p^{Red}). Both $V^{V/IV}$ and $W^{VI/V}$ processes display similar trends in ΔE_p in the order $[EMIM]^+ \approx [BMIM]^+ > [Py_{14}]^+ \approx [TEA]^+ > [TPA]^+ > [TBA]^+ > [THA]^+$. Notable, ΔE_p values associated with the $V^{V/IV}$ process changes gradually, with the lowest and highest values being 63 and 110 mV for $[EMIM]^+$ and $[THA]^+$, respectively, whereas, in the case of the $W^{VI/V}$ process, ΔE_p changes significantly when changing the electrolyte cation from $[TEA]^+$ to $[TPA]^+$, $[TBA]^+$ and $[THA]^+$, with values of 67, 303, 520 and 745 mV, respectively. Even after considering differences in the uncompensated resistance (R_u) (*e.g.*, R_u = 415 and 1153 Ω with $[EMIM]^+$ and $[THA]^+$, respectively), a smaller ΔE_p reflects a larger k^0 value, as described in the classical theoretical treatment of dc cyclic voltammetric *I-E* curves by Nicholson and Shain.[44] This indicates that the kinetics of the $V^{V/IV}$ and $W^{VI/V}$ processes are electrolyte cation dependent in PC, as noted in other media.[36] Moreover, the

kinetics of the $W^{VI/V}$ process appear to be more sensitive to the nature of electrolyte compared to the $V^{V/IV}$ one.

Full details of the E_F^0 and ΔE_p values associated with the $V^{V/IV}$ and $W^{VI/V}$ processes in the different electrolyte media at a Pt electrode, along with the separation between the E_F^0 values associated with the two processes (ΔE_F^0) are provided in Table 1. Finally, diffusion coefficients (*D*) calculated from the Randles-Sevcik relationship[35] based on the peak current associated with the reversible $V^{V/IV}$ process at a GC macrodisk electrode,[36] are included in Table 2. Interestingly, the value of *D* decreases by about 70% when changing the electrolyte cation from $[EMIM]^+$ to $[THA]^+$. The diffusion coefficient is governed by the Stokes-Einstein relationship[45],

$$D = \frac{k_B T}{6\pi\eta a} \tag{8}$$

where k_B is the Boltzmann constant, η is the viscosity of the medium and a is the hydrodynamic radius of the diffusing particle. Clearly, according to this equation, the value of *D* depends on the viscosity of the media as well as the size of the ion paired $[SVW_{11}O_{40}]^{3-}$. If it is assumed that the size term (a) is independent on the nature of electrolyte, the *D* value of each electrolyte medium is expected to be inversely proportional to η values of corresponding media and the produced [$D \cdot \eta$] is expected to be constant. However, there is no such relationship between *D* and η values as shown in Table 2. On this basis, both the size of the ion paired $[SVW_{11}O_{40}]^{3-}$ and viscosity are believed to contribute to difference in *D* values.

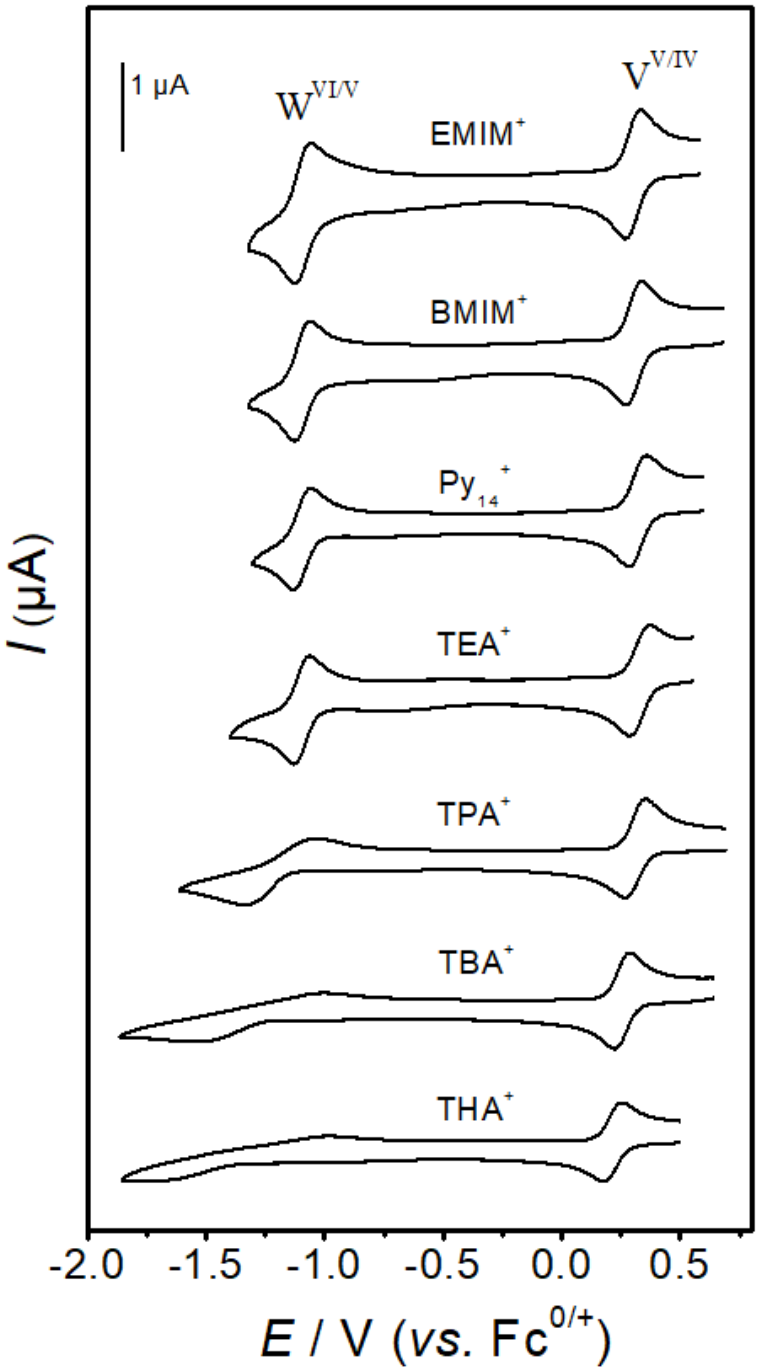

Figure 2. Dc cyclic voltammograms obtained at a Pt macrodisk electrode (v = 0.1 V s^{-1}) from the reduction of $[SVW_{11}O_{40}]^{3-}$ in PC containing 0.5 M electrolyte with constituent cations (from top to bottom) $[EMIM]^+$, $[BMIM]^+$, $[Py_{14}]^+$, $[TEA]^+$, $[TPA]^+$, $[TBA]^+$ and $[THA]^+$.

Table 2. Summary of the D values for the reduction of 1.0 mM $[SVW_{11}O_{40}]^{3-}$ in PC (0.5 M electrolyte) at a Pt macrodisk (diameter = 1.0 mm) electrode.

Electrolyte	η (cP)	D ($\times 10^6$ cm^2 s^{-1})	$[D\cdot\eta]$ ($\times 10^{13}$ m kg s^{-2})
[EMIM][BF_4]	3.07	1.3	4.0
[BMIM][BF_4]	3.21	1.1	3.5
[Py_{14}][BF_4]	3.44	0.93	3.2
[TEA][BF_4]	3.12	0.93	2.9
[TPA][BF_4]	3.58	0.77	2.8
[TBA][PF_6]	3.90	0.60	2.3
[THA][ClO_4]	4.98	0.42	2.1

Determination of k^0 for fast processes by FTAC Voltammetry and slow ones by DC cyclic voltammetry. The k^0 values associated with the $V^{V/IV}$ (k_V^0) and $W^{VI/V}$ (k_W^0) processes in PC containing 0.5 M electrolyte were determined at a Pt macrodisk electrode by FTAC voltammetry using a sine wave perturbation (ΔE = 80 mV and f = 9.02 Hz or 27.01 Hz) and scanning the DC potential over the range where both the $V^{V/IV}$ and $W^{VI/V}$ reduction processes are present in the voltammogram. The parameters used in the simulations to define the electron transfer process, E^0, k^0, α, electrode area (A), R_u and double-layer capactitance (C_{dl}), were derived using the Bulter-Volmer model of electron transfer as described in the Supporting Information and are provided in Table 1 and 3. Since the electrode kinetics of the $V^{V/IV}$ and $W^{VI/V}$ processes in PC containing [EMIM][BF_4] and [BMIM][BF_4] are essentially reversible with a frequency of 9.02 Hz, a higher frequency (f = 27.01 Hz) AC perturbation was used to shorten the time scale of the measurement so that adequate kinetic sensitivity was available. A representative FTAC voltammogram (f = 27.01 Hz) obtained in PC containing [EMIM][BF_4] as the supporting electrolyte is shown in Figure 3. For the other four electrolytes (see Table 1), the $V^{V/IV}$ and $W^{VI/V}$ processes were found to be far from reversible allowing the lower frequency of 9 Hz to be used to quantify the electrode kinetics. A representative FTAC

voltammogram (f = 9.02 Hz) obtained in PC containing [TPA][BF_4] as the supporting electrolyte is shown in Figure 4.

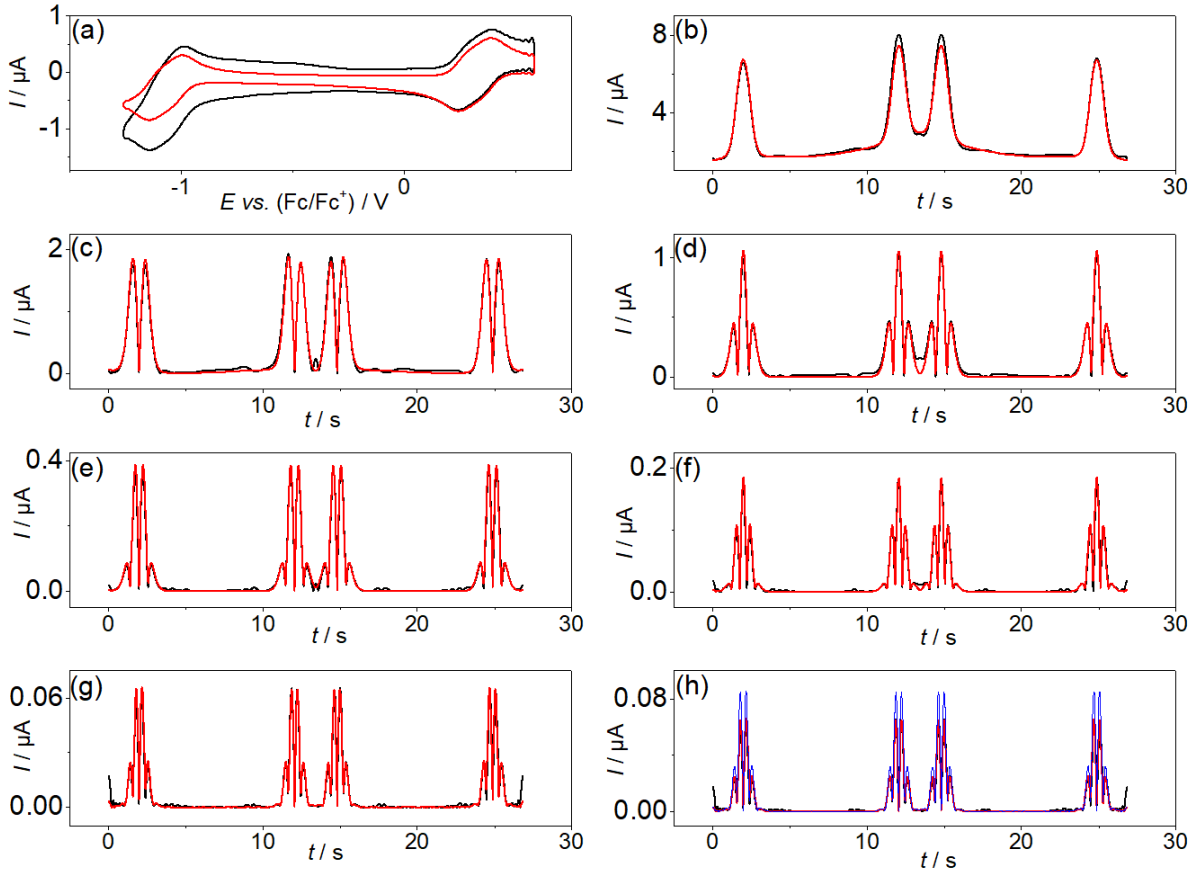

Figure 3. Comparison of simulated (—) and experimental (—) FTAC voltammetric data obtained for the $V^{IV/V}$ and $W^{VI/V}$ processes in PC containing 1.0 mM $[SVW_{11}O_{40}]^{3-}$ and 0.5 M [EMIM][BF_4] at a 1 mm diameter Pt macrodisk electrode with T = 295 K, ΔE = 80 mV, f = 27.01 Hz and v = 0.137 V s^{-1}. (a) aperiodic DC component, (b–g) 1st to 6th AC harmonic components, and (h) simulated 6th harmonic component for the reversible case (—). Simulated kinetic data was obtained with k^0_V = 0.10 cm s^{-1}, α_V = 0.50, k^0_W = 0.10 cm s^{-1} and α_W = 0.50. Other parameters are defined in the text.

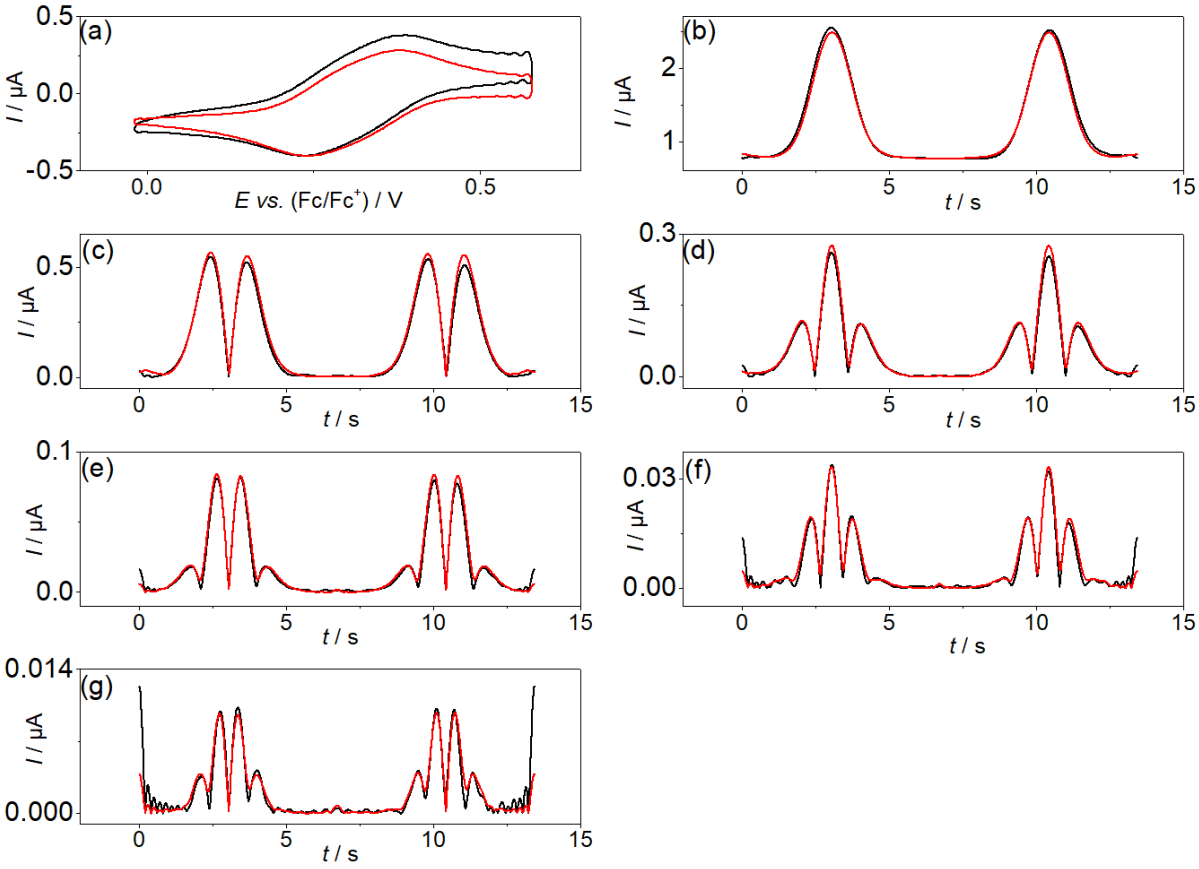

Figure 4. Comparison of simulated (—) and experimental (—) FTAC voltammetric data obtained for the $V^{IV/V}$ process in PC containing 1.0 mM $[SVW_{11}O_{40}]^{3-}$ and 0.5 M $[TPA][BF_4]$ at a 1 mm diameter Pt electrode with T = 295 K, ΔE = 80 mV, f = 9.02 Hz and v = 0.089 V s^{-1}. (a) aperiodic DC component, (b–g) 1st to 6th AC harmonic components. Simulated kinetic data was obtained with k_V^0 = 0.0075 cm s^{-1}, α_V = 0.5 were used. Other parameters are defined in the text.

Figure 3 provides a simulation-experiment comparison for the $V^{V/IV}$ and $W^{VI/V}$ processes in PC containing 0.5 M [EMIM][BF_4]. In the 6th harmonic component, both processes can be treated as quasi-reversible rather than reversible on this timescale (see Figure 3h), since the current magnitude for this harmonic is significantly smaller than predicted for a reversible process (blue curve). Excellent agreement between the simulated and experimental data was achieved for all harmonic components with k_V^0 and k_W^0 both estimated to be 0.10 cm s^{-1}. α was reasonally assumed to be 0.50 in all simulations in accordance with the highly symmetric shapes of all AC harmonics.

Since the electrode kinetics of the $W^{VI/V}$ process when using [TPA][BF_4], [TBA][PF_4] and [THA][ClO_4] as the electrolyte are so slow, higher order harmonic components are almost absent, only the narrowed potential range associated with the $V^{V/IV}$ process was quantified by FTACV under these conditions. The FTAC voltammogram (f = 9.02 Hz) obtained for the $V^{V/IV}$ process in PC containing 0.5 M [TPA][BF_4] is shown in Figure 4. Excellent agreement between the simulated and experimental data was achieved using the measured A, D, C and R_u values to give a k_V^0 value of 0.0075 cm s^{-1}. For the $W^{VI/V}$ process, it should be noted that when using [TPA][BF_4], [TBA][PF_4] and [THA][ClO_4] as the electrolyte, the DC cyclic voltammograms obtained from the first cycling scan give larger peak-to-peak separations than those obtained from the following ones. Furthermore, the shapes of the reduction and oxidation peaks are not fitted perfectly with simulated ones obtained based on Butler-Volmer theory (Figure S1(a)). For slow electrode kinetics such as the $W^{VI/V}$ process, the differences between Butler-Volmer theory and Marcus-Hush theory in simulation are expected to be distinguishable. Better fitting was found when comparing the experimental data and simulated one based on Marcus-Hush theory (Figure S1(b)). However, a large deviation between experimental and simulated data still exists. All the discussions above indicate there are complexities associated with the $W^{VI/V}$ process when using [TPA][BF_4], [TBA][PF_4] and

[THA][ClO_4] as the electrolyte. Therefore, in this study the electrode kinetics of this process were estimated by comparing the peak-to-peak separations of the experimental DC cyclic voltammograms obtained from the first cycling scan with those obtained by DigiElch digital simulation based on Butler-Volmer theory, taking into account the effect of uncompensated resistance (R_u). A k_W^0 value of 1.2×10^{-4} cm s^{-1} was estimated when using [THA][ClO_4] as the electrolyte. The heterogeneous electron transfer kinetics of the $V^{V/IV}$ and $W^{VI/V}$ processes were measured in PC with the 7 different electrolytes outlined in Scheme 1; the FTAC voltammetric data obtained for $[BMIM]^+$, $[Py_{14}]^+$, $[TEA]^+$, $[TBA]^+$ and $[THA]^+$ are included in the Supporting Information (see Figures S2 to S6) and the measured k^0 values are summarized in Table 3.

FTAC voltammetric data were also acquired with a lower bulk concentration of 0.20 mM $[SVW_{11}O_{40}]^{3-}$ in order to lessen the influence of the IR_u drop. The results obtained at a Pt macrodisk electrode in PC (0.5 M electrolyte) at this lower bulk concentration are also summarized in Table 3. Comparisons of experimental and simulated data are presented in Figures S7 to S13 in the Supporting Information. As expected, since the IR_u drop has been correctly accommodated for in all simulations, the determined k^0 values are essentially independent of the $[SVW_{11}O_{40}]^{3-}$ concentration. This concentration independence also implies that the contribution from specific adsorption is not significant.

The data summarized in Table 3 reveal that k_V^0 and k_W^0 are both affected by the nature of the supporting electrolyte, with increasing size of the electrolyte cation causing a decrease in the measured value. For example, for the $V^{V/IV}$ process, k^0 decreases by approximately three orders of magnitude when the electrolyte cation is changed from $[EMIM]^+$ to $[THA]^+$. As discussed previously,[36] the length of the imidazolium based cations ($[EMIM]^+$ and $[BMIM]^+$) are similar to the diameter of ammonium based cations ($[TPA]^+$ or $[TBA]^+$). However, the planar structure of imidazolium based-cation is thought to cause its preferred

orientation to be parallel rather than perpendicular to the electrode surface. With this in mind, we can conclude that the k_V^0 values are dependent on the size of the electrolyte cation, decreasing in the order; $[EMIM]^+ > [BMIM]^+ > [Py_{14}]^+ \approx [TEA]^+ > [TPA]^+ > [TBA]^+ > [THA]^+$. The same trend in k^0 is also observed for the $W^{VI/V}$ process, however with a more significant decrease (approximately two orders of magnitude) from $[TEA]^+$ to $[TPA]^+$, namely, $[EMIM]^+ > [BMIM]^+ > [Py_{14}]^+ \approx [TEA]^+ >> [TPA]^+ > [TBA]^+ > [THA]^+$. It should be noted that the impact of the thermodynamically favourable cross redox reaction between $[SVW_{11}O_{40}]^{3-}$ and $[SVW_{11}O_{40}]^{5-}$ on the voltammetric characteristics is insignificant, as demonstrated in a previous study.[35]

Table 3. Electrode kinetic parameters derived at a 1 mm dimeter Pt macrodisk electrode for the $[SVW_{11}O_{40}]^{3-/4-/5-}$ processes in PC (0.5 M electrolyte).

Electrolyte	C (mM)	R_u[a] (Ω)	C_{dl}[a] (c_0, c_1, c_2, c_3, c_4) (μF cm^{-2})	E_V^0 (V)	k_V^0 (cm s^{-1})	E_W^0 (V)	k_W^0 (cm s^{-1})
$[EMIM][BF_4]$	1.0	415	16.1, -2.1, -5.3, -4.9, -1.1	0.316	0.10	-1.085	0.10
	0.20	430	13.2, 1.5, 6.1, 4.8, 1.4		0.10		0.10
$[BMIM][BF_4]$	1.0	535	20.9, 0.2, -4.0, -4.3, -1.2	0.306	0.040	-1.093	0.038
	0.20	515	14.6, 1.0, -1.5, -3.6, -1.3		0.050		0.045
$[Py_{14}][BF_4]$	1.0	470	28.5, 0.5, -4.5,-3.7, -0.9	0.333	0.016	-1.079	0.016
	0.20	502	14.3, 0.7, 0.2, -0.1, -0.1		0.018		0.017
$[TEA][BF_4]$	1.0	550	31.2, -2.8, -16.9, -14.6, -3.9	0.342	0.015	-1.079	0.020
	0.20	543	16.0, 1.11, -2.9, -4.3, -1.4		0.012		0.020
$[TPA][BF_4]$	1.0	530	21.5, -0.6, 8.2, 28.8, 24.5	0.309	0.0075	-1.182	1.2×10^{-4}[b]
	0.20	630	13.4, 0.6, -0.2, 8.0, 12.3		0.0085		c
$[TBA][PF_6]$	1.0	730	22.0, -0.5, 10.1, 7.3, -12.4	0.254	0.0040	-1.260	1.2×10^{-5}[b]
	0.20	750	12.4, 1.1, -4.1, 7.0, 19.5		0.0033		c
$[THA][ClO_4]$	1.0	1330	12.0, -0.5, 10.1, 7.2, -12.4	0.214	0.0018	-1.355	1.7×10^{-6}[b]
	0.20	1270	13.9, 2.4, 0.6, -3.1, -1.1		0.0016		c

[a] See supporting information for detailed measurement.
[b] Estimated from ΔE_p values obtained from DC cyclic voltammetry.
[c] No well-defined process observed at this lower concentration.
[d] FTACV simulations were obtained assuming $\alpha = 0.50$.

The solvent chosen in this study, PC, has a relatively high dielectric constant (64.9 at 25 °C[42]), which is expected to minimise the extent of ion pairing. For example, a measurable amount of ion pairing between the electrolyte cation and nitromesitylene radicals has been reported in acetonitrile and dimethylformamide[46] (with dielectric constants of 36 and 36.7, respectively), while negligible ion pairing between the same anion radical and the electrolyte cation has been suggested in PC.[47] Nevertheless, owing to the high negative charge of POM anions, the occurrence of electrolyte cation-POM ion pairing in the present study is expected (the electrolyte cation dependence of the E^0 values (see Table 3) implies that ion pairing is significant). In this case, the electrode kinetics have been measured at apparent formal potentials (E^0_{app}) rather than formal potential E^0_{F}, so k^0 should be more appropriately considered as an apparent rate constant (k^0_{app}). In this situation, the kinetics of the overall electron transfer reaction scheme can be described by the square reaction given in Eq. 3,

$$\begin{array}{ccc} \mathrm{A} + \mathrm{e}^- & \rightleftharpoons & \mathrm{B} \quad (E_1{}^0, k_1{}^0) \\ K_1 \Big\updownarrow & & \Big\updownarrow K_2 \\ \mathrm{XA}^+ + \mathrm{e}^- & \rightleftharpoons & \mathrm{XB}^+ \quad (E_2{}^0, k_2{}^0) \end{array} \qquad (3)$$

In this scheme, the symbols A and B are used to represent $[SVW_{11}O_{40}]^{3-}$ and $[SVW_{11}O_{40}]^{4-}$, respectively so that $K_1 = \frac{[X^+][A]}{[XA^+]}$ and $K_2 = \frac{[X^+][B]}{[XB^+]}$ are the equilibrium constants for the ion-pairing reactions involving either the oxidised or the reduced forms, $E_1{}^0$ and $E_2{}^0$ are the relevant formal potentials and; $k_1{}^0$ and $k_2{}^0$ are the formal electron transfer rate constants at $E_1{}^0$ and $E_2{}^0$, respectively. It can be shown that the voltammetric responses associated with this process are

identical to a simple one-electron transfer process in Eq. 4 if the ion pairing reactions are reversible on the voltammetric timescale.

$$A' + e^- \rightleftharpoons B' \quad (k_{app}{}^0, \alpha_{app}, E_{app}{}^0) \tag{4}$$

where

$$k_{\mathrm{app}}{}^0 = \frac{k_1{}^0(K_2/K_1)^{\alpha_{app}} + k_2{}^0([\mathrm{X}^+]/K_1)}{[1+([\mathrm{X}^+]/K_1)]^{1-\alpha_{\mathrm{app}}}[(K_2/K_1)+([\mathrm{X}^+]/K_1)]^{\alpha_{\mathrm{app}}}} \tag{5}$$

Since a higher charge density is associated with the species B, K_2 is expected to be smaller than K_1. It is also reasonable to assume that both K_1 and K_2 are smaller than unity due to relatively strong association between highly charged POMs and electrolyte cations. Consequently, the relationships $K_2/K_1 \ll [X^+]/K_1$ and $k_1{}^0(K_2/K_1)^{1/2} \ll k_2{}^0([X^+]/K_1)$ are expected to be valid under the experimental conditions employed as noted in other studies.[48, 49] On this basis, Eq. 5 can be simplified to give Eq. 6 with α_{app} taken to be 0.5,

$$k_{\mathrm{app}}{}^0 = \frac{k_1{}^0(K_2/K_1)^{1/2} + k_2{}^0([\mathrm{X}^+]/K_1)}{[1+([\mathrm{X}^+]/K_1)]^{1/2}[(K_2/K_1)+([\mathrm{X}^+]/K_1)]^{1/2}} \approx \frac{k_2{}^0([\mathrm{X}^+]/K_1)^{1/2}}{[1+([\mathrm{X}^+]/K_1)]^{1/2}}$$

$$= \frac{k_2{}^0}{[1+(K_1/[X^+])]^{1/2}} \tag{6}$$

As the size of the cation increase ($[TEA]^+ > [TPA]^+ > [TBA]^+ > [THA]^+$), the ion pairs formation become weaker and K_1 is expected to increase. Assuming $k_2{}^0$ is insensitive to the identity of the electrolyte cation, $k_{app}{}^0$ is therefore predicted to decrease in the order of $[TEA]^+ > [TPA]^+ > [TBA]^+ > [THA]^+$.

The apparent formal potentials E^0_{app} is also a function of E^0_1, K_1, K_2 and $[X^+]$ [49]

$$(F/RT)(E^0_{\mathrm{app}} - E^0_1) = \ln\left[\frac{1+([\mathrm{X}^+]/K_1)}{1+([\mathrm{X}^+]/K_2)}\right] \tag{7}$$

Rearrangement gives

$$(F/RT)(E^0_{\mathrm{app}} - E^0_1) = \ln\left(\frac{K_2+[\mathrm{X}^+]}{K_1+[\mathrm{X}^+]} \cdot \frac{K_1}{K_2}\right) \tag{8}$$

As K_1 and K_2 are much smaller than 1, it is reasonable to assume $\frac{K_2+[X^+]}{K_1+[X^+]} \approx 1$. Therefore,

$$(F/RT)(E^0_{\text{app}} - E^0_1) \approx \ln(\frac{K_1}{K_2}) \qquad (9)$$

When the electrolyte cation is small, ion pair formation is stronger, and the difference between K_1 and K_2 is larger than that when using a larger cation. Since K_1 is expected to be larger than K_2 as explained above, the values of $\ln(\frac{K_1}{K_2})$ are predicted to increase with the size of electrolyte cation which decrease in the order $[THA]^+ < [TBA]^+ < [TPA]^+ < [TEA]^+$. Consequently, on the basis of Eq. (9), we can deduce that E^0_{app} values are expected to follow the order $[THA]^+ < [TBA]^+ < [TPA]^+ < [TEA]^+$. Figure 5 provides a plot of k^0_{app} values associated with the $V^{V/IV}$ and $W^{VI/V}$ processes as a function of their formal reversible potential, which indeed confirms k^0_{V} and k^0_{W} values decrease, and the E^0_V and E^0_W shift towards more negative potentials as the size of electrolyte cations increase as predicted. However, ion pairing cannot be the sole reason for the electrolyte cation dependence of the k^0 values, as this does not account for the dramatically different k^0_{V} and k^0_{W} dependence on supporting electrolyte.

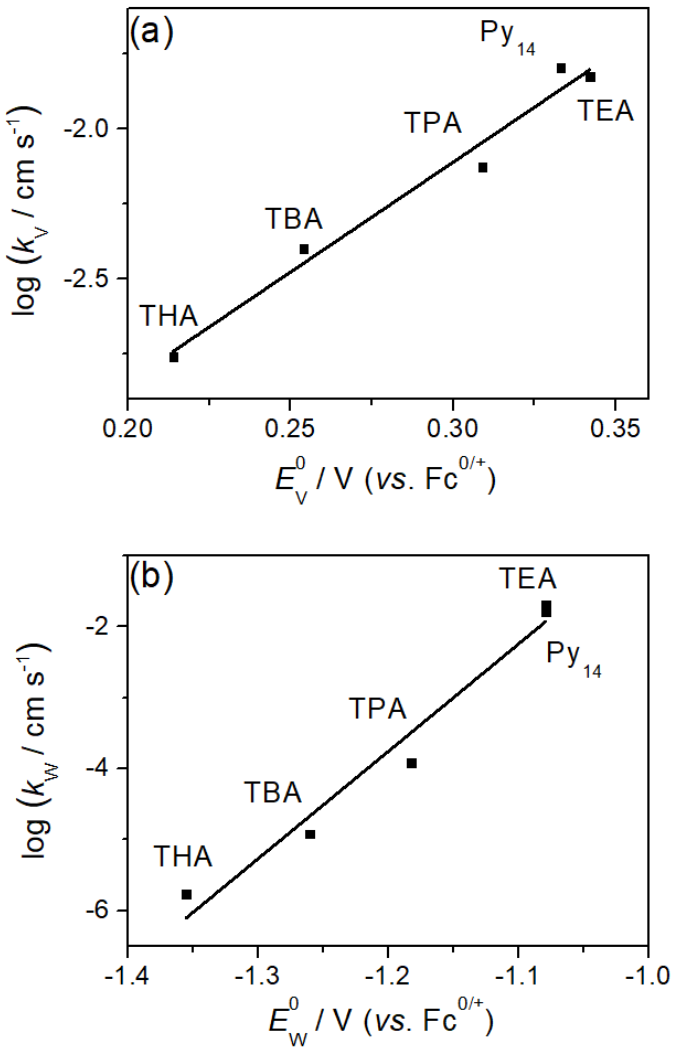

Figure 5. Plots of the logarithm of k^0 for the (a) $V^{V/IV}$ and (b) $W^{VI/V}$ processes *vs*. formal reversible potential in PC containing 0.5 M electrolyte.

In the Marcus Theory of electron transfer, the heterogeneous rate constant associated with a simple outer sphere electrode process is inverse proportional to the activation Gibbs energy, ΔG^*.[14] The total activation energy ΔG^* can be divided into inner ΔG_i^* and outer ΔG_o^* components of the reorganization energies. The inner component of reorganization energy reflects the bonds between the centered metal and the ligands. The outer component of reorganization energy corresponds to the interaction of the complex with the molecules or ions in the medium. Considering the structure of the POM remains similar after electron transfer, it

is reasonable to assume that ΔG_o^* makes a dominanth contribution. On this basis, the k^0 values are expected to descrease with increase in the viscosity of the solvent (electrolyte), which is the case for both k_V^0 and k_W^0 when the electrolyte cation is changed from $[TEA]^+$ to $[THA]^+$. However, the viscosity of PC containing 0.5 M [TEA][BF_4] is only 1.5 times smaller than that containing 0.5 M [THA][ClO_4], while the k_V^0 values decrease approximately by a factor of 10 and k_W^0 values decrease more significantly (approximately four orders of magnitude). Therefore, the contribution from media change in viscosity are not the major factor.

Significant electrolyte cation dependence of the k^0 values also may arise from specific adsorption of $[SVW_{11}O_{40}]^{3-}$, $[SVW_{11}O_{40}]^{4-}$ and/or $[SVW_{11}O_{40}]^{5-}$. However, since the k_V^0 and k_W^0 values found at the two $[SVW_{11}O_{40}]^{3-}$ concentrations (1 mM and 0.2 mM) are almost identical, a specific adsorption effect is unlikely, as this is expected to give rise to concentration dependence.

In general, if it is assumed that the reaction plane is coincident with the outer Helmholtz plane, the electrolyte cation dependence of k^0 may be consequence of the double layer effect.[50] However, as highlighted in previous studies, it appears that the double layer effect alone cannot account for the magnitude of the electrolyte cation size effect observed herein. Gamber, et al.[51] found that at negative potentials, tetraalkylammonium cations are adsorbed at a mercury electrode/electrolyte interface in acetonitrile, with the extent of adsorption becoming more extensive with increasing length of the constituent alkyl chain of the cation. Evans, et al.[52] studied the inhibiting effect of large tetraalkylammonium cations on the electrode kinetics for a wide variety of electrode reactions. In their study, these authors showed that the k^0 values became smaller when $[THA]^+$ replaced $[TEA]^+$ as the electrolyte cation. This suggested that at negative potentials, the electrode is extensively covered with adsorbed tetraalkylammonium cations and therefore k^0 electrolyte dependence was explained in terms of blockage of electron transfer by the concentrated “film” of tetraalkylammonium cations.

Simply, it can be assumed that $d = 2r_+$ (d is the thickness of the "film" and r_+ is the diameter of the electrolyte cation). However, since the alkyl arms of the larger tetraalkylammonium cations (n ≥ 3) can bend under the influence of an electric field, the charge center at the nitrogen atom is able to approach the surface at a distance of 0.37 nm.[47] This necessitate the introduction of correction factor to the thickness of the "film" for the larger tetraalkylammonium cations:[47]

$$d = 2r_+ \qquad n \leq 3 \tag{10}$$

$$d = r_+ + 0.37 \qquad n \leq 3 \tag{11}$$

Table 4 shows the crystallographic radius (r_+) and the calculated thickness of the coverage (d) for each of the tetraalkylammonium cations. A plot of $\ln k_0$ measured in PC solutions containing the range tetraalkylammonium cations used versus d (calculated using Eqs. 10 and 11) is shown in Figure 6. Reasonable linear correlations (r^2 = 0.99 and 0.98 for $V^{V/IV}$ and $W^{VI/V}$ processes, respectively) between are obtained for both the $V^{V/IV}$ and $W^{VI/V}$ processes.

In our previous studies,[35,36] the electrode kinetics of $V^{V/IV}$ and $W^{VI/V}$ processes were found to be dependent on the electrode material, which is consistent with the prediction of Marcus theory. In Marcus theory, the adsorbed layers on the electrode/electrolyte interface can impede electron transfer.[50, 53-55] When electron tunneling occurs from an electrode which is covered by an adsorbed layer to a redox active species in the solution phase, the standard rate constant is proportional to thickness of adsorbed layer:[47]

$$k^0 = k^{0\prime} e^{-\beta d} \tag{12}$$

where $k^{0'}$ is the standard rate constant for the uncovered electrode and β is the tunneling parameter. Reasonable linear correlations between $\ln k_0$ and d were obtained for both $V^{V/IV}$ and $W^{VI/V}$ processes, which is consistent with that predicted by Marcus theory. The slopes of the plots, which are equivalent to β (see Eq. 12), are found to be 13.3 nm^{-1} for the $V^{V/IV}$ process

and 58.9 nm^{-1} for the $W^{VI/V}$ process, which suggests the latter has a higher barrier height. Lipkowski et al.,[53] who studied the electrode kinetics of redox processes at mercury electrodes coated with monolayers of quinolone, iso-quinoline and 3-methyl-iso-quinoline found that the monolayers existed as concentrated liquid-like films or compact solid-like films depending on the magnitude of the electrode potential. While the former has a significant inhibitive effect, the latter can decelerate the electrode reaction much more effectively, by up to 6-7 orders of magnitude. On this basis, the results in our study can be attribute in part to inhibiting effect of adsorbed tetraalkylammonium cations on the electrode surface that form a blocking layer which reduces the probability of electron transfer through the layer; the thickness of the layer increases with the size of electrolyte cation. In the potential region where the $V^{V/IV}$ process occurs (close to the potential of zero charge, pzc), the monolayer acts as a liquid-like film, and as a result, the k_V^0 values decrease gently with an increase in the electrolyte cation size. For the $W^{VI/V}$ process, which appears in a much more negative potential region (significantly negative of the pzc), the monolayer becomes more compact and acts as a solid-like film, particularly when using the larger tetraalkylammonium cations. Consequently, a more significant drop in k_W^0 is observed when changing the electrolyte cation from $[TEA]^+$ to $[TPA]^+$, $[TBA]^+$ and $[THA]^+$.

Although the dimensions of $[EMIM]^+$ and $[BMIM]^+$ are known, it is problematic to estimate the thickness of the layer for these two cations, since these center of charge is able to approach the electrode surface at a closer distance than spherical ammonium cations, due to their planar structure. For this reason, k^0 data for these two cations are not included in the plot shown in Figure 6. However, it is important to note that comparison of these k^0 values also reveals a decrease with increase in the length of the alkyl chain (see Table 3). Furthermore, given that the structure of $[Py_{14}]^+$ is similar to that of $[TEA]^+$, in terms of the length of the alkyl groups, comparable k^0 values are expected when using these two cations, as observed

experimentally (k_V^0 = 0.016 cm s^{-1}, k_W^0 = 0.016 cm s^{-1} with $[Py_{14}]^+$ and k_V^0 = 0.015 cm s^{-1}, k_W^0 = 0.02 cm s^{-1} with $[Py_{14}]^+$). On the basis of the above analysis, the observed cation dependent k_V^0 and k_W^0 (Figure 6) is consistent with the prediction based on the Marcus theory.

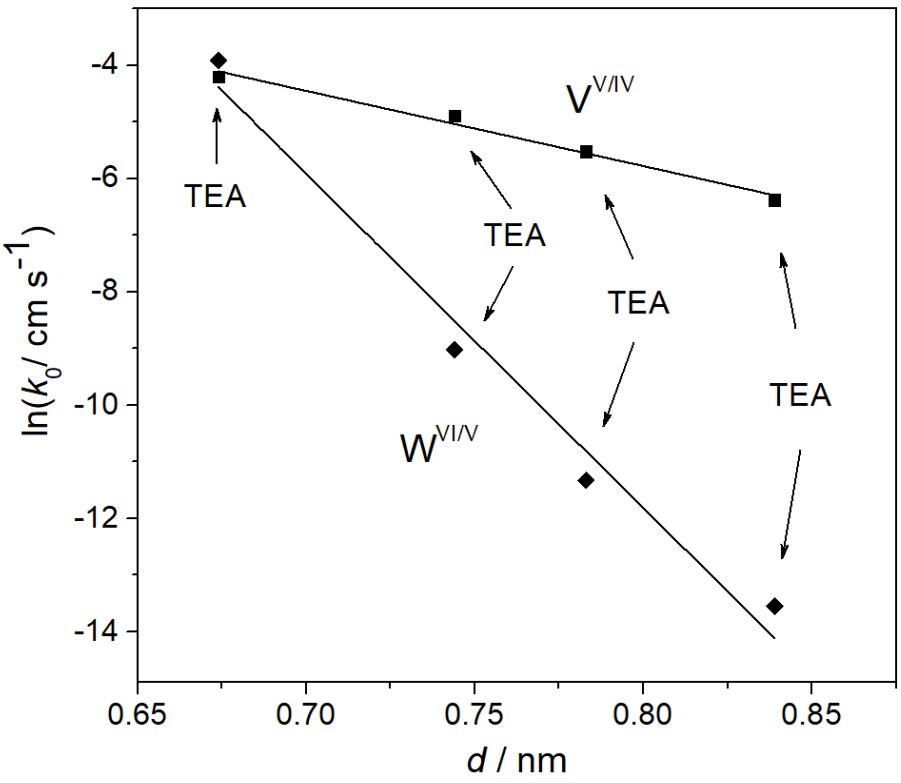

Figure 6. Plot of the natural logarithm of k^0 for the $V^{V/IV}$ (■) and $W^{VI/V}$ (◆) processes measured at a Pt electrode in the presence of designated tetraalkylammonium cations versus the thickness of the coverage (*d*), calculated from the crystallographic radius of the relative cations (see Eqs. 11 and 12).

Table 4. Cation Crystallographic radii (r_+) and calculated thickness of the coverage (*d*) of the tetraalkylammonium cations employed in this study.

Electrolyte	Cation crystallographic radius r_+ (nm)[56]	Thickness of the coverage *d* (nm)
$[TEA][BF_4]$	0.337	0.674
$[TPA][BF_4]$	0.372	0.744
$[TBA][PF_6]$	0.413	0.783

[THA][ClO_4]	0.469	0.839

Conclusions

The heterogeneous electron transfer kinetics associated with the $[SVW_{11}O_{40}]^{3-/4-/5-}$ processes at a platinum electrode have been investigated in PC containing seven different supporting electrolyte cations using large amplitude FTAC voltammetry to quantify very fast kinetics and DC cyclic voltammetry for slow kinetics. The formal reversible potentials and electron-transfer rate constants associated with the $V^{V/IV}$ and $W^{VI/V}$ processes were found to correlate with the size of the supporting electrolyte cation. k^0 values decrease in the order, $[EMIM]^+ > [BMIM]^+ > [Py_{14}]^+ \approx [TEA]^+ > [TPA]^+ > [TBA]^+ > [THA]^+$ for both processes even though they occur at very different potentials, and while k_V^0 decreases more gently with increasing cation size, changing by approximately three orders of magnitude, the decrease in k_W^0 is more drastic, changing by approximately five orders of magnitude from $[EMIM]^+$ to $[THA]^+$. Possible explanations for the electrolyte cation depedence were considered (*e.g.*, ion-pairing, viscosity, adsorption and the double-layer effect), with inhibition of electron-transfer by a blocking "film" of electrolyte cations being proposed as the dominant factor, supported by the linear plot of $\ln(k^0)$ vs. $\ln(d)$ for both the $V^{V/IV}$ and $W^{VI/V}$ electron transfer processes. The nature of the cation "film" is thought to change from liquid-like (moderately inhibiting) in the potential region where the $V^{V/IV}$ process occurs, to solid-like (strongly inhibiting) in the potential region where the $W^{VI/V}$ process occurs, thereby explaining the different sensitivities of the respective processes to the nature of the supporting electrolyte cations.

Acknowledgements

J.L. acknowledges Monash University for provision of postgraduate publication award support. The authors also gratefully acknowledge the Australian Research Council for financial support.

References

[1] J. Velmurugan, P. Sun, M.V. Mirkin, Scanning electrochemical microscopy with gold nanotips: the effect of electrode material on electron transfer rates, The Journal of Physical Chemistry C, 113 (2008) 459-464.

[2] R.K. Jaworski, R.L. McCreery, Laser activation of carbon microdisk electrodes: Surface oxide effects on $Ru(NH_3)_6^{3+/2+}$ kinetics, Journal of Electroanalytical Chemistry, 369 (1994) 175-181.

[3] Z. Samec, J. Weber, The effect of the double layer on the rate of the Fe^{3+}/Fe^{2+} reaction on a platinum electrode and the contemporary electron transfer theory, Journal of Electroanalytical Chemistry and Interfacial Electrochemistry, 77 (1977) 163-180.

[4] C.A. McDermott, K.R. Kneten, R.L. McCreery, Electron Transfer Kinetics of Aquated $Fe^{3+/2+}$, $Eu^{3+/2+}$ and $V^{3+/2+}$ at Carbon Electrodes Inner Sphere Catalysis by Surface Oxides, Journal of The Electrochemical Society, 140 (1993) 2593-2599.

[5] S. Sahami, M.J. Weaver, Solvent effects on the kinetics of simple electrochemical reactions: Part I. Comparison of the behavior of Co (III)/(II) trisethylenediamine and ammine couples with the predictions of dielectric conitnuum theory, Journal of Electroanalytical Chemistry and Interfacial Electrochemistry, 124 (1981) 35-51.

[6] A. Kapturkiewicz, B. Behr, Solvent effect on electrode reaction kinetics of transition metal salene complexes, Journal of electroanalytical chemistry and interfacial electrochemistry, 179 (1984) 187-199.

[7] G.E. McManis, M.N. Golovin, M.J. Weaver, Role of solvent reorganization dynamics in electron-transfer processes. Anomalous kinetic behavior in alcohol solvents, The Journal of Physical Chemistry, 90 (1986) 6563-6570.

[8] K. Hsueh, E. Gonzalez, S. Srinivasan, Electrolyte effects on oxygen reduction kinetics at platinum: a rotating ring-disc electrode analysis, Electrochimica Acta, 28 (1983) 691-697.

[9] C. Beriet, D. Pletcher, A microelectrode study of the mechanism and kinetics of the ferro/ferricyanide couple in aqueous media: The influence of the electrolyte and its concentration, Journal of Electroanalytical Chemistry, 361 (1993) 93-101.

[10] S.K. Cook, B.R. Horrocks, Heterogeneous Electron- Transfer Rates for the Reduction of Viologen Derivatives at Platinum and Bismuth Electrodes in Acetonitrile, ChemElectroChem, DOI (2016).

[11] T. Iwasita, W. Schmickler, J. Schultze, The influence of metal adatoms deposited at underpotential on the kinetics of an outer-sphere redox reaction, Journal of electroanalytical chemistry and interfacial electrochemistry, 194 (1985) 355-359.

[12] T. Iwasita, W. Schmickler, J. Schultze, The influence of the metal on the kinetics of outer sphere redox reactions, Berichte der Bunsengesellschaft für physikalische Chemie, 89 (1985) 138-142.

[13] M.J. Weaver, T. Gennett, Influence of solvent reorientation dynamics upon the kinetics of some electron-exchange reactions, Chemical physics letters, 113 (1985) 213-218.

[14] C. Lagrost, L. Preda, E. Volanschi, P. Hapiot, Heterogeneous electron-transfer kinetics of nitro compounds in room-temperature ionic liquids, Journal of Electroanalytical Chemistry, 585 (2005) 1-7.

[15] M.D. Ryan, D.H. Evans, Effect of metal ions on the electrochemical reduction of benzil in non-aqueous solvents, Journal of Electroanalytical Chemistry and Interfacial Electrochemistry, 67 (1976) 333-357.

[16] M. Ryan, D.H. Evans, Effect of Sodium Ions on the Electrochemical Reduction of Diethyl Fumarate in Dimethylsulfoxide and Acetonitrile, Journal of The Electrochemical Society, DOI (1974).

[17] M.J. Hazelrigg, A.J. Bard, Electrohydrodimerization Reactions IV. A Study of the Effect of Alkali Metal Ions on the Hydrodimerization of Several 1, 2- Diactivated Olefins in DMF Solutions by Chronoamperometry and Chronocoulometry, Journal of The Electrochemical Society, 122 (1975) 211-220.
[18] W. Fawcett, A. Lasia, The influence of ion pairing on the electroreduction of nitromesitylene in aprotic solvents. 2. Kinetic aspects, The Journal of Physical Chemistry, 82 (1978) 1114-1121.
[19] R. Andreu, J.J. Calvente, W.R. Fawcett, M. Molero, Role of ion pairing in double-layer effects at self-assembled monolayers containing a simple redox couple, The Journal of Physical Chemistry B, 101 (1997) 2884-2894.
[20] M. Peover, J. Davies, The influence of ion-association on the polarography of quinones in dimethylformamide, Journal of Electroanalytical Chemistry (1959), 6 (1963) 46-53.
[21] M.T. Pope, A. Müller, Polyoxometalate chemistry: an old field with new dimensions in several disciplines, Angewandte Chemie International Edition in English, 30 (1991) 34-48.
[22] D.-L. Long, E. Burkholder, L. Cronin, Polyoxometalate clusters, nanostructures and materials: from self assembly to designer materials and devices, Chemical Society Reviews, 36 (2007) 105-121.
[23] P. Special, issue: L. Cronin and A. Müller (guest eds.), Chem. Soc. Rev, 41 (2012) 7325-7648.
[24] M.V. Vasylyev, R. Neumann, New heterogeneous polyoxometalate based mesoporous catalysts for hydrogen peroxide mediated oxidation reactions, Journal of the American Chemical Society, 126 (2004) 884-890.
[25] K. Kamata, K. Yonehara, Y. Sumida, K. Yamaguchi, S. Hikichi, N. Mizuno, Efficient epoxidation of olefins with≥ 99% selectivity and use of hydrogen peroxide, Science, 300 (2003) 964-966.
[26] H. Lü, J. Gao, Z. Jiang, F. Jing, Y. Yang, G. Wang, C. Li, Ultra-deep desulfurization of diesel by selective oxidation with $[C_{18}H_{37}N(CH_3)_3]_4[H_2NaPW_{10}O_{36}]$ catalyst assembled in emulsion droplets, Journal of Catalysis, 239 (2006) 369-375.
[27] C.L. Hill, Progress and challenges in polyoxometalate-based catalysis and catalytic materials chemistry, Journal of Molecular Catalysis A: Chemical, 262 (2007) 2-6.
[28] M. Sadakane, E. Steckhan, Electrochemical properties of polyoxometalates as electrocatalysts, Chemical Reviews, 98 (1998) 219-238.
[29] M. Zhou, L.P. Guo, F.Y. Lin, H.X. Liu, Electrochemistry and electrocatalysis of polyoxometalate-ordered mesoporous carbon modified electrode, Analytica chimica acta, 587 (2007) 124-131.
[30] Z. Han, Y. Zhao, J. Peng, Y. Feng, J. Yin, Q. Liu, The electrochemical behavior of Keggin polyoxometalate modified by tricyclic, aromatic entity, Electroanalysis, 17 (2005) 1097-1102.
[31] K.K. Kasem, Electrochemical behavior of sodium 12-tungstodicobaltoate in aqueous and mixed solvent electrolytes, Electrochimica acta, 41 (1996) 205-211.
[32] K. Maeda, S. Himeno, T. Osakai, A. Saito, T. Hori, A voltammetric study of Keggin-type heteropolymolybdate anions, Journal of Electroanalytical Chemistry, 364 (1994) 149-154.
[33] K. Bano, J. Zhang, A.M. Bond, P.R. Unwin, J.V. Macpherson, Diminished Electron Transfer Kinetics for $[Ru(NH_3)_6]^{3+/2+}$, $[\alpha\text{-}SiW_{12}O_{40}]^{4-/5-}$ and $[\alpha\text{-}SiW_{12}O_{40}]^{5-/6-}$ Processes at Boron-Doped Diamond Electrodes, The Journal of Physical Chemistry C, 119 (2015) 12464-12472.
[34] J. Li, A.M. Bond, J. Zhang, Probing Electrolyte Cation Effects on the Electron Transfer Kinetics of the $[\alpha\text{-}SiW_{12}O_{40}]^{4-/5-}$ and $[\alpha\text{-}SiW_{12}O_{40}]^{5-/6-}$ Processes using a Boron-Doped Diamond Electrode, Electrochimica Acta, 178 (2015) 631-637.
[35] J. Li, S.-X. Guo, C.L. Bentley, K. Bano, A.M. Bond, J. Zhang, T. Ueda, Electrode Material Dependence of the Electron Transfer Kinetics Associated with the $[SVW_{11}O_{40}]^{3-/4-}$ ($V^{V/IV}$) and

[$SVW^{11}O^{40}]^{4-/5-}$ ($W^{VI/V}$) Processes in Dimethylformamide, Electrochimica Acta, 201 (2016) 45-56.
[36] J. Li, C.L. Bentley, A.M. Bond, J. Zhang, T. Ueda, Influence of 1-butyl-3-methylimidazolium on the electron transfer kinetics associated with the $[SVW_{11}O_{40}]^{3-/4-}$ ($V^{V/IV}$) and [$SVW^{11}O^{40}]^{4-/5-}$ ($W^{VI/V}$) processes in dimethylformamide, Journal of Electroanalytical Chemistry, DOI (2016).
[37] T. Ueda, J.-i. Nambu, J. Lu, S.-X. Guo, Q. Li, J.F. Boas, L.L. Martin, A.M. Bond, Structurally characterised vanadium (v)-substituted Keggin-type heteropolysulfates $[SVM_{11}O_{40}]^{3-}$ (M= Mo, W): voltammetric and spectroscopic studies related to the V (v)/V (iv) redox couple, Dalton Transactions, 43 (2014) 5462-5473.
[38] A. Baranski, W. Fawcett, Medium effects in the electroreduction of cyanobenzenes, Journal of Electroanalytical Chemistry and Interfacial Electrochemistry, 100 (1979) 185-196.
[39] D.A. Corrigan, D.H. Evans, Cyclic voltammetric study of tert-nitrobutane reduction in acetonitrile at mercury and platinum electrodes: Observation of a potential dependent electrochemical transfer coefficient and the influence of the electrolyte cation on the rate constant, Journal of Electroanalytical Chemistry and Interfacial Electrochemistry, 106 (1980) 287-304.
[40] C. Rüssel, W. Jaenicke, Heterogeneous electron transfer to quinones in aprotic solvents: Part II. The dependence on solvent and supporting electrolyte, Journal of electroanalytical chemistry and interfacial electrochemistry, 180 (1984) 205-217.
[41] A. Kapturkiewicz, M. Opałło, Medium effect in the electroreduction of nitromesitylene, Journal of electroanalytical chemistry and interfacial electrochemistry, 185 (1985) 15-28.
[42] J. Barthel, F. Feuerlein, Dielectric properties of propylene carbonate and propylene carbonate solutions, Journal of solution chemistry, 13 (1984) 393-417.
[43] A.M. Bond, D. Elton, S.-X. Guo, G.F. Kennedy, E. Mashkina, A.N. Simonov, J. Zhang, An integrated instrumental and theoretical approach to quantitative electrode kinetic studies based on large amplitude Fourier transformed ac voltammetry: A mini review, Electrochemistry Communications, 57 (2015) 78-83.
[44] R.S. Nicholson, Theory and Application of Cyclic Voltammetry for Measurement of Electrode Reaction Kinetics, Analytical Chemistry, 37 (1965) 1351-1355.
[45] C.C. Miller, The Stokes-Einstein Law for diffusion in solution, Proceedings of the Royal Society of London. Series A, Containing Papers of a Mathematical and Physical Character, 106 (1924) 724-749.
[46] B. Chauhan, W. Fawcett, A. Lasia, The influence of ion pairing on the electroreduction of nitromesitylene in aprotic solvents. 1. Thermodynamic aspects, The Journal of Physical Chemistry, 81 (1977) 1476-1481.
[47] W.R. Fawcett, M. Fedurco, M. Opallo, The inhibiting effects of tetraalkylammonium cations on simple heterogeneous electron transfer reactions in polar aprotic solvents, The Journal of Physical Chemistry, 96 (1992) 9959-9964.
[48] Y. Liu, S.-X. Guo, A.M. Bond, J. Zhang, Y.V. Geletii, C.L. Hill, Voltammetric Determination of the Reversible Potentials for $[\{Ru_4O_4(OH)_2(H_2O)_4\}(\gamma\text{-}SiW_{10}O_{36})_2]^{10-}$ over the pH Range of 2–12: Electrolyte Dependence and Implications for Water Oxidation Catalysis, Inorganic chemistry, 52 (2013) 11986-11996.
[49] S.-X. Guo, S.W. Feldberg, A.M. Bond, D.L. Callahan, P.J. Richardt, A.G. Wedd, Systematic Approach to the Quantitative Voltammetric Analysis of the FeIII/FeII Component of the $[\alpha_2\text{-}Fe(OH_2)P_2W_{17}O_{61}]^{7-/8-}$ Reduction Process in Buffered and Unbuffered Aqueous Media, The Journal of Physical Chemistry B, 109 (2005) 20641-20651.
[50] D.H. Evans, A.G. Gilicinski, Comparison of heterogeneous and homogeneous electron-transfer rates for some nitroalkanes and diketones, The Journal of Physical Chemistry, 96 (1992) 2528-2533.

[51] R. Gambert, H. Baumgärtel, The influence of cations on the interface between the mercury electrode and non-aqueous CH_3CN, Journal of electroanalytical chemistry and interfacial electrochemistry, 183 (1985) 315-328.
[52] R.A. Petersen, D.H. Evans, Heterogeneous electron transfer kinetics for a variety of organic electrode reactions at the mercury-acetonitrile interface using either tetraethylammonium perchlorate or tetraheptylammonium perchlorate electrolyte, Journal of electroanalytical chemistry and interfacial electrochemistry, 222 (1987) 129-150.
[53] J. Lipkowski, C. Buess-Herman, J. Lambert, L. Gierst, Mechanism of electron transfer through monomolecular films of neutral organic species adsorbed at an electrode surface, Journal of electroanalytical chemistry and interfacial electrochemistry, 202 (1986) 169-189.
[54] C. Miller, P. Cuendet, M. Graetzel, Adsorbed. omega.-hydroxy thiol monolayers on gold electrodes: evidence for electron tunneling to redox species in solution, The Journal of Physical Chemistry, 95 (1991) 877-886.
[55] H.O. Finklea, D.D. Hanshew, Electron-transfer kinetics in organized thiol monolayers with attached pentaammine (pyridine) ruthenium redox centers, Journal of the American Chemical Society, 114 (1992) 3173-3181.
[56] Y. Marcus, J. Chipperfield, Ionic solvation: Wiley-Interscience, Chichester, 1985 (ISBN 0-471-90756-1). viii+ 306 pp, Elsevier, 1986.